Application of Photonic Crystal Enhanced Fluorescence to a Cytokine Immunoassay

Patrick C. Mathias,[†] Nikhil Ganesh,[‡] and Brian T. Cunningham*,[§]

Nano Sensors Group, Micro and Nanotechnology Laboratory, University of Illinois at Urbana–Champaign, 208 North Wright Street, Urbana, Illinois 61801

Photonic crystal surfaces are demonstrated as a means for enhancing the detection sensitivity and resolution for assays that use a fluorescent tag to quantify the concentration of an analyte protein molecule in a liquid test sample. Computer modeling of the spatial distribution of resonantly coupled electromagnetic fields on the photonic crystal surface are used to estimate the magnitude of enhancement factor compared to performing the same fluorescent assay on a plain glass surface, and the photonic crystal structure is fabricated and tested to experimentally verify the performance using a sandwich immunoassay for the protein tumor necrosis factor-alpha (TNF-α). The demonstrated photonic crystal fabrication method utilizes a nanoreplica molding technique that allows for large-area inexpensive fabrication of the structure in a format that is compatible with confocal microarray laser scanners. The signal-to-noise ratio for fluorescent spots on the photonic crystal is increased by at least 5-fold relative to the glass slide, allowing a TNF-α concentration of 1.6 pg/mL to be distinguished from noise on a photonic crystal surface. In addition, the minimum quantitative limit of detection on the photonic crystal surface is one-third the limit on the glass slide—a decrease from 18 to 6 pg/mL. The increased performance of the immunoassay allows for more accurate quantitation of physiologically relevant concentrations of TNF-α in a protein microarray format that can be expanded to multiple cytokines.

The simultaneous quantitation of multiple proteins promises to aid researchers seeking to understand protein interaction networks and may potentially be clinically useful for diagnosis and prognosis with serum biomarkers.[1] One approach to multiplexed protein detection has been an adaptation of the DNA microarray format to immunoassays. Fluorescence-based protein microarrays have demonstrated detection limits comparable to their enzyme-based counterparts, enzyme linked immunosorbent assays (ELISA), while measuring multiple proteins within each array. These protein microarrays have been adapted and optimized for detection of cancer biomarkers[2] and cytokines.[3–5] Cytokines are a particularly promising class of analytes for multiplexed detection because they rarely act alone and rely on the upregulation or downregulation of multiple cytokines simultaneously to achieve a particular physiological effect. Cytokines are associated with immune responses to infection, but may be associated with noninfectious diseases. Because the immune system is integrated with other physiological systems such as the cardiovascular and gastrointestinal systems, and cytokines often act as a signaling system throughout the body, these proteins may be a valuable tool in understanding and diagnosing disease. While protein microarrays on optically passive surfaces such as glass slides have been useful in multiplexed cytokine quantitation, the utility of these arrays can be expanded by a more accurate determination of protein levels as well as lowered limits of detection. In this work, we demonstrate how photonic crystal (PC) surfaces can be used to achieve improved detection sensitivity and more accurate quantification of a representative protein biomarker compared to performing the same immunoassay on a glass surface.

The PCs used in this work are nanostructures composed of a periodically modulated low refractive index plastic/SiO$_2$ surface structure that is coated with a high refractive index dielectric. The purpose of the structure is to provide an efficient optical resonator, as described in previous research,[6–9] but summarized briefly here. The periodically modulated dielectric structure of the PC functions as a reflective optical filter. Only particular wavelength/incident angle combinations interact strongly with the structure, resulting in highly efficient reflection, while all other wavelength/incident angle combinations are transmitted through. Unlike a conventional diffraction grating, only the zeroth-order reflected and transmitted waves can propagate, while higher order modes are cut off. However, the PC supports leaky eigenmodes

* To whom correspondence should be addressed. E-mail: bcunning@ illinois.edu.
† Department of Bioengineering.
‡ Department of Material Science and Engineering.
§ Department of Electrical and Computer Engineering.

(1) Kingsmore, S. F. *Nature Reviews Drug Discovery* **2006,** *5,* 310–321.
(2) Woodbury, R. L.; Varnum, S. M.; Zangar, R. C. *J. Proteome Res.* **2002,** *1,* 233–237.
(3) Li, Y.; Reichert, W. M. *Langmuir* **2003,** *19,* 1557–1566.
(4) Saviranta, P.; Okon, R.; Brinker, A.; Warashina, M.; Eppinger, J.; Geier-stanger, B. H. *Clin. Chem.* **2004,** *50,* 1907–1920.
(5) Kusnezow, W.; Syagailo, Y. V.; Ruffer, S.; Baudenstie, N.; Gauer, C.; Hoheisel, J. D.; Wild, D.; Goychuk, I. *Mol. Cell. Proteomics* **2006,** *5,* 1681–1696.
(6) Mathias, P. C.; Ganesh, N.; Chan, L. L.; Cunningham, B. T. *Appl. Opt.* **2007,** *46,* 2351–2360.
(7) Ganesh, N.; Zhang, W.; Mathias, P. C.; Chow, E.; Soares, J. A. N. T.; Malyarchuk, V.; Smith, A. D.; Cunningham, B. T. *Nat. Nanotechnol.* **2007,** *2,* 515–520.
(8) Ganesh, N.; Mathias, P. C.; Zhang, W.; Cunningham, B. T. *J. Appl. Phys.* **2008,** *103,* 083104.
(9) Mathias, P. C.; Ganesh, N.; Zhang, W.; Cunningham, B. T. *J. Appl. Phys.* **2008,** *103,* 094320.

to which higher diffracted orders can couple through phase-matching. The leaky eigenmodes reradiate into the reflected direction in phase with the reflected zeroth-order wave, leading to constructive interference. Likewise, the leaky eigenmode reradiation into the transmitted direction is out of phase with the transmitted zeroth-order wave, resulting in destructive interference.[10] This phenomenon is observed under broadband illumination as a highly efficient reflection at a wavelength that fulfills the phase-matching criteria, referred to as the resonant wavelength. The phase-matching condition is also dependent on the incident angle of the external illumination, so each incident angle can have one or more distinct resonant wavelengths. This resonance effect, termed guided-mode resonance, has been exploited to design highly efficient narrowband optical filters[11] as well as label-free optical biosensors.[12]

The leaky eigenmodes are highly localized within and in direct proximity to the PC surface, and a large energy density is observed at these locations in the form of enhanced electromagnetic fields throughout the structure. The intensity of a fluorophore's emission is proportional to the electric field intensity (which is proportional to the square of the electric field) of the light exciting the molecule, so an enhanced electric field will enhance the excitation of fluorophores close to the device surface. Enhanced excitation works selectively in regions within proximity to the PC surface due to an exponential decay in the electric field intensity from the PC into the superstrate (region above the PC). Thus, enhanced excitation of the PC shares one of the advantages of total internal reflection fluorescence (TIRF) microscopy because fluorophores close to the substrate surface are selectively excited.[13] Rather than utilizing a TIRF microscope, a conventional confocal microarray scanner can be utilized for rapid imaging of large areas. Using PC-enhanced excitation, we have demonstrated fluorescence enhancement from the fluorescent dye Cyanine-5[6] (Cy5) and detailed the spectral characteristics of the PC-fluorophore interaction[9] as well as the dependence on distance from the PC on enhanced excitation.[8]

While enhanced excitation can be observed when the laser light incident on the PC is spectrally aligned with the resonance wavelength, another enhancement effect can be observed when the fluorophore emission wavelengths overlap the resonant wavelengths of the PC. Enhanced extraction occurs when light emitted by fluorophores couples into leaky eigenmodes and is reradiated such that it can be easily detected by the measurement instrumentation. Essentially, the PC causes some proportion of photons that would normally radiate through the substrate to be reoriented toward the direction of incident light. Because the same optics that illuminate the sample are responsible for collecting emitted light, this phenomenon allows a higher proportion of the emitted photons to be measured relative to a passive substrate such as glass. PCs are designed to exhibit resonances at an excitation wavelength close to the emission wavelength (typically within 50-nm wavelength); because the resonances continuously span many wavelengths over a range of angles, the eigenmodes
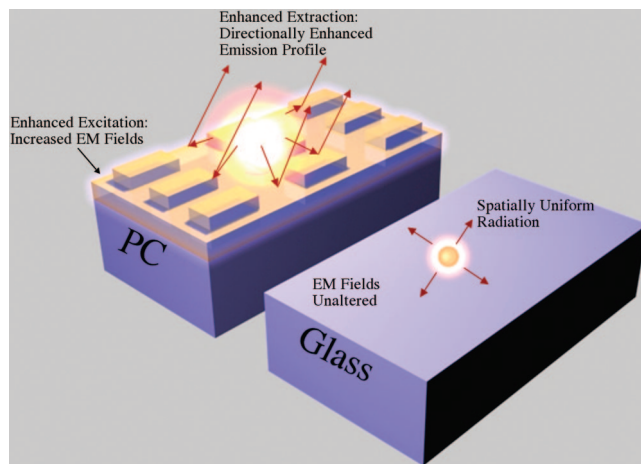

Figure 1. Schematic of enhanced fluorescence mechanisms observed on the photonic crystal (PC). When the laser excitation wavelength aligns with the PC resonance wavelength, enhanced electromagnetic (EM) fields are observed throughout the PC. This enhanced excitation effect will excite fluorophores more strongly than if they were situated above an optically passive structure such as glass. Furthermore, if the fluorophore emission wavelengths overlap the PC resonance wavelengths, light emitted from fluorophores can be redirected toward the photon detection instrumentation, which is the basis of enhanced extraction.

will overlap both the excitation and the emission wavelengths. Thus, a PC designed for enhanced excitation will perform enhanced extraction as well, and both effects are summarized in Figure 1. The combination of these two effects has been used to enhance the fluorescence from semiconductor quantum dots[7] with a magnification factor of 8× for the excitation effect and 13× for the extraction effect, for an overall sensitivity enhancement of 108×.

In this work, we perform a microspot fluorescence immunoassay for the cytokine protein tumor necrosis factor-alpha (TNF-α) simultaneously on glass slides and PC surfaces under identical experimental conditions to evaluate the impact of enhanced fluorescence on the assay. The PC used in this work is similar to a combined label-free biosensor and enhanced fluorescence device described previously.[6] While this PC is capable of label-free detection of proteins that could enable spot density quantitation, we focus on the impact of enhanced fluorescence on the signal-to-noise ratio (SNR) of the assay since this can allow more accurate quantitation of protein levels at the lowest concentrations assayed. The optical properties of the PC are explored by computer modeling to predict the magnitude of the enhanced excitation effect and for comparison with experimental measurements. Using a nanoreplica molding process, PCs the size of microscope slides are fabricated for compatibility with commercial microarray spotters and scanners. A layer of SiO_2 is added to the PC so an identical surface chemistry interaction can be achieved on both the PC and the glass slide. A microspot immunoassay is performed on both substrates using a fluorescent Cyanine-5 label. By evaluating the immunoassay over a concentration series on glass and PCs, the impact of PC enhanced fluorescence on the assay resolution and detection limit is assessed.

MATERIALS AND METHODS

Reagents. (3-Glycidoxypropyl)trimethoxysilane (GPTS), phosphate-buffered saline (PBS) powder, glycerol, Tween-20, and

(10) Rosenblatt, D.; Sharon, A.; Friesem, A. A. *IEEE J. Quantum Electron.* **1997**, *33*, 2038–2059.

(11) Wang, S. S.; Magnusson, R. *Appl. Opt.* **1993**, *32*, 2606–2613.

(12) Cunningham, B. T.; Li, P.; Lin, B.; Pepper, J. *Sens. Actuators, B* **2002**, *81*, 316–328.

(13) Sutherland, R. M.; Dahne, C.; Place, J. F.; Ringrose, A. R. *J. Immunol. Methods* **1984**, *74*, 253–265.

bovine serum albumin (BSA) were purchased from Sigma-Aldrich. Glass microscope slides and acetic acid were purchased from Fischer Scientific. Ethanol (200 proof) was purchased from Decon Laboratories, Inc. Phosphate-Buffered Saline Milk Blocking Solution was purchased from BioFX Laboratories. The capture antibody (Mab1), biotinylated detection antibody (Mab11), and recombinant TNF-α were all purchased from BioLegend. Cyanine-5 conjugated streptavidin was purchased from GE Healthcare. The spotting buffer used to dilute the capture antibody was 5% glycerol in PBS. The TNF-α and detection antibody were diluted in 1% BSA in PBS. The Cy5-conjugated streptavidin was diluted in 0.05% Tween in PBS (PBS-T). All wash steps were performed with PBS-T.

Device Simulation. Rigorous coupled-wave analysis (RCWA)[14] was employed to simulate the behavior of the PC under multiple illumination conditions. Simulations were performed with commercial software (R-Soft DiffractMOD) that modeled the transmission characteristics under broadband illumination as well as the electric field profiles for the structure at resonance when illuminated with a 633-nm source. The three-dimensional spatial distribution of electric field intensities within the PC structure at resonance were derived from the square of the three-dimensional electric field profile output from the software.

Device Fabrication and Characterization. The PCs were fabricated by a nanoreplica molding process described previously.[15] Briefly, a silicon wafer "master" mold template consisting of a negative volume image of the PC grating pattern was fabricated by deep-UV lithography. UV-curable polymer was sandwiched between the master and a flexible sheet of poly(ethylene terephthalate) (PET), and the polymer was cured to a solid phase using a high-intensity UV lamp. The replica was peeled from the master and a layer of SiO_2 was deposited by sputtering to separate the high refractive index layer from the autofluorescent UV-cured polymer. The high refractive index layer of TiO_2 was then deposited by sputtering to complete the PC. A thin film of SiO_2 (15 nm) was deposited onto the PC in order to provide a surface equivalent to a glass slide for the silane surface chemistry. PC slides were created by cutting the replicated sheet to a 1 in. × 3 in. area and mounting it to a microscope slide with optically clear adhesive film (3M). The surface structure was characterized with an atomic force microscope (Dimension 3000, Digital Instruments). Optical characterization of PCs was carried out by illumination of the devices with a collimated, polarized white light source and collection of transmitted light into a UV–vis light spectrometer (USB 2000 Ocean Optics, Inc.). PC slides were mounted onto a rotational stage and rotated in order to ascertain the angle at which the device would exhibit a resonance at a laser illumination wavelength of 633 nm.

Surface Chemistry. An epoxysilane-based surface chemistry selected for providing a low degree of background autofluorescence was utilized.[16] Glass slide control substrates were first washed by immersion in 0.1 M NaOH for 1 h, followed by a 15-min ultrasonication in the same solution. Glass slides and PC slides were treated for 5 min in an O_2 plasma (Texas Instruments

Planar Plasma System). The same surface treatment was then applied to both types of slides. Slides were immersed in a solution consisting of 10 mM acetic acid in ethanol with 2.5% GPTS for 1 h. The slides were then washed twice with ethanol and dried under a nitrogen stream.

Immunoassay Protocol. Twelve 9×9 mm^2 wells were drawn onto each slide with a hydrophobic pen (Super HT Pap Pen, Research Products International Corp.). Nine spots of capture antibody (Mab1) at a concentration of 250 μg/mL in the 5% glycerol spotting buffer were applied to each well using a noncontact droplet deposition instrument (Perkin-Elmer Piezoarray). After spotting, the slides were stored at 4 °C overnight. The slides were washed by immersion in water and blocked with PBS Milk Blocking Solution for 1 h. The slides were then washed with PBS-T and a concentration series of TNF-α was applied to each slide for 2 h. Five concentrations and one negative control in duplicate were added to the wells of the slides, with a maximum concentration of 1 ng/mL diluted 5-fold to a minimum concentration of 1.6 pg/mL. After washing, detection antibody (biotin−Mab11) was added to each well at a concentration of 10 μg/mL for 1 h. Cy5-conjugated streptavidin was then added at a concentration of 10 μg/mL for 30 min. Slides were washed and dried under a stream of nitrogen.

Fluorescence Detection and Analysis. Fluorescence measurements were taken using a commercially available confocal microarray scanner with user-adjustable angle of incidence laser excitation (LS Reloaded, Tecan) in order to allow alignment of the PC resonance with the incident wavelength. The PC slides and glass slides were scanned with identical conditions (photomultiplier tube (PMT) gain, incidence angle). PC slides were scanned at an angle that fulfills the resonant condition at 633 nm (3.2°) and an angle at which no resonance occurs at this wavelength (20°). Array Pro Analyzer software was used to quantify spot and background fluorescent intensities. ImageJ software was used to generate spatial profiles of the fluorescence data. ProMAT (http://www.pnl.gov/statistics/ProMAT) was used to fit fluorescence data to a four-parameter logistic model and to calculate the lower limit of detection for the immunoassay.

RESULTS

Device Simulation and Characterization. The PC used in this work has a structure similar to the polarization-dependent combined enhanced fluorescence and label-free biosensing PC previously designed and tested by our group.[6] However, in that work, the PC was fabricated by electron beam lithography over an area of only 1 mm^2; we have modified the design and employed an 8-in. silicon master wafer to inexpensively fabricate the PC over large areas using a nanoreplica molding approach, as described in Materials and Methods. Thus, PC surfaces may be produced to cover the entire surface of conventional microscope slides for compatibility with the liquid handling and scanning instrumentation methods typically used for microarrays.

The PC structure, shown in Figure 2a, is composed of a UV-cured polymer (not pictured), a SiO_2 layer that is refractive index-matched to the polymer ($n_{SiO_2} = 1.45$) and a high-refractive index TiO_2 layer ($n_{TiO_2} = 2.35$). The PC has a different grating period in each of the two orthogonal axes along the surface, with a period of $\Lambda_y = 535$ nm in one direction, a period $\Lambda_x = 365$ nm in the other direction, and a structure height of $d = 40$ nm. The incident

(14) Moharam, M. G.; Gaylord, T. K. *J. Opt. Soc. Am.* **1981**, *71*, 811–818.
(15) Cunningham, B.; Lin, B.; Qiu, J.; Li, P.; Pepper, J.; Hugh, B. *Sens. Actuators. B* **2002**, *85*, 219–226.
(16) Kusnezow, W.; Jacob, A.; Walijew, A.; Diehl, F.; Hoheisel, J. D. *Proteomics* **2003**, *3*, 254–265.
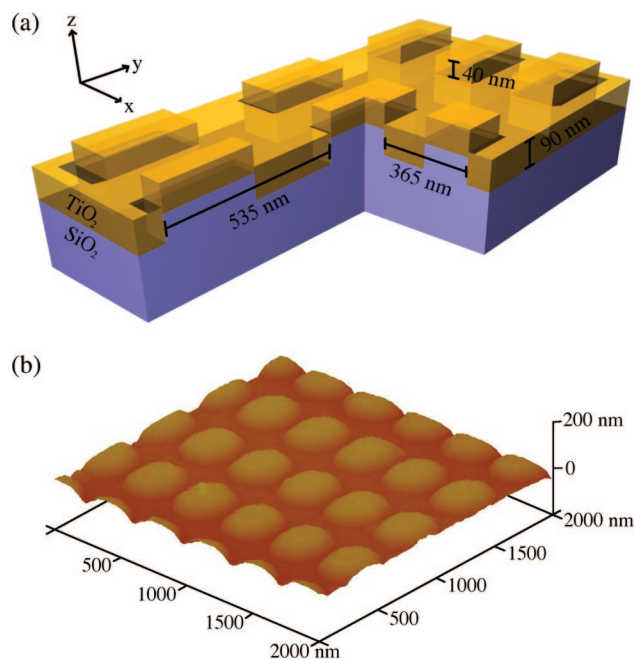
Figure 2. (a) Simulation model of the photonic crystal. External laser illumination polarized in the *y*-direction interacts with the structure, resulting in electric field enhancement. (b) Atomic force micrograph of the fabricated photonic crystal. The measured period in the *x*-direction is 360 nm, the period in the *y*-direction is 520 nm, and the height of the structure is 45 nm.

light illuminating the structure has its electric field polarization in the *y*-direction. For this simulation, the *y*-axis is defined as the rotation axis for the incident light. The simulation does not take into account any rounding of the structures that may occur during fabrication, nor does it account for slight differences in deposited film thickness on the upper and lower horizontal surfaces that may occur during sputtering. As is apparent from the atomic force microscope image in Figure 2b, significant rounding is observed in the final replicated PC structure since the flux of the sputtered molecules is not completely normal to the surface during the deposition process. The measured periods are $\Lambda_y = 520$ nm and $\Lambda_x = 360$ nm, while the measured structure height is $d = 45$ nm.

The guided-mode resonance that amplifies the electric field near the PC surface is observable as a highly efficient reflection at the necessary combination of wavelength and incident angle of external light. The incident angle required to achieve a guided-mode resonance at the HeNe laser wavelength ($\lambda = 633$ nm) can be ascertained through measurements of white light transmission through the PC. Figure 3a shows simulated and measured transmission intensity as a function of wavelength for an incident angle that results in a resonance condition at a wavelength of $\lambda = 633$ nm. The simulated PC exhibited this resonance when the incident angle was tuned to 4.1°, while the actual PC had a resonance angle of 4.2°. Both transmission dips for the measured and the simulated structures lie at similar values, 633 and 678 nm, showing excellent agreement between the theoretically modeled and experimentally observed behavior. It is important to note that the dip at 678 nm lies within the range of the emission filter (and fluorophore emission wavelengths) for the microarray scanner used in this work (690 ± 20 nm). In fact, the resonance will overlap these wavelengths for a range of incident angles, so
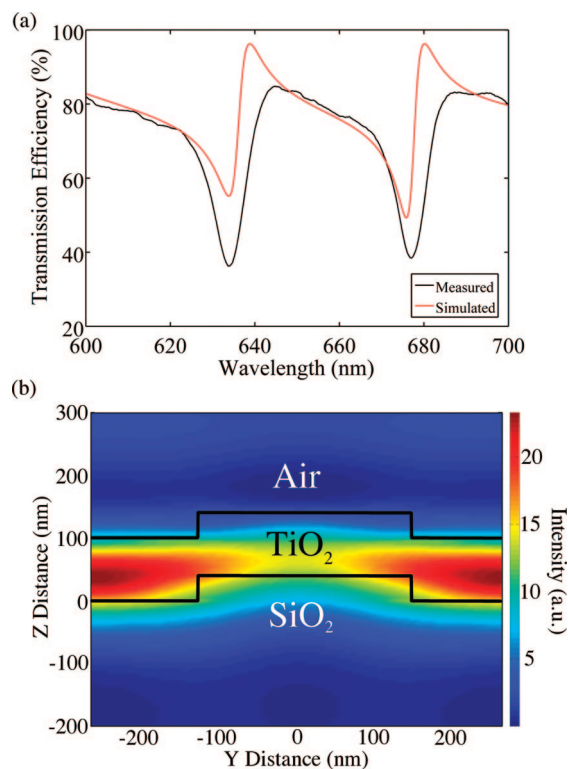
Figure 3. (a) Transmission efficiency as a function of wavelength for the simulated and fabricated photonic crystal. The angle of incidence for both structures was adjusted so the device is resonant at 633 nm. The angle of incidence for the simulated structure was 4.1°, and the angle of incidence for the actual device was 4.2°. (b) Electric field intensity cross section plotted for one period of the device. The maximum field intensity is 22 times the incident field intensity. An exponential decay of the intensity can be observed from the top of the structure into the air superstrate.

that enhanced extraction of Cyanine-5 fluorescence may be observed, in addition to enhanced excitation due to the 633-nm resonance.

The electric fields within the structure under resonant illumination are enhanced relative to the incident electric field, leading to enhanced excitation of fluorophores in proximity to the high-field region. To quantify this effect, electric field intensities were derived from the simulation during illumination with polarized, $\lambda = 633$-nm light. A plot of one cross section of the total simulated electric field intensities in the PC is shown in Figure 3b. The electric field intensity shown in this plot represents one period of the device in one lateral direction, or a distance of 535 nm. The electric field intensities are also periodically spaced in the other lateral direction at a period 360 nm (not shown). The highest electric field intensity, ~22× the incident light intensity, appears within the high refractive index TiO$_2$ layer, and evanescently decays into the air medium above the PC surface. The average electric field intensity on the top exposed surface of the PC (including the added SiO$_2$ layer) is ~7× the intensity of incident light, which suggests that fluorophores directly on the PC would exhibit a fluorescence intensity that is up to seven times higher than on an optically passive substrate (due to the effect of enhanced excitation alone). However, it is unlikely fluorescent tags used in a sandwich ELISA assay would be present directly upon the PC surface due to surface chemistry layers, the immobilized antibody layer, and the analyte layer and are thus

most likely to be found up to 20 nm above the SiO$_2$ surface. The average electric field intensity 20 nm above the PC surface is ∼4× the incident intensity, so a fluorescence excitation enhancement of between 4× and 7× can be expected from the effects of enhanced electric fields with the present structure.

Raw Fluorescence Intensity Data. For the purposes of quantifying the effect of the PC on the measured fluorescence intensity images, clear distinctions between measured quantities within this microspot assay should be made. Measurements of fluorescent intensity outside of the immunoassay spots are referred to as background intensity, and each spot has an associated local background intensity. These background intensities have some distribution associated with random noise, so noise is defined as the standard deviation of the background intensity. The fluorescence intensity from each spot is the raw signal intensity, but more important for our analysis is the net signal intensity, which is the background-subtracted raw signal intensity.

The PC can influence the intensity of Cyanine-5 fluorescence by the two previously described effects: enhanced excitation and enhanced extraction. These effects can be separated by illuminating the structure with incident light at the $\lambda = 633$ nm resonant angle, which will be referred to as the PC "on-resonance", and illuminating the structure with light at another arbitrary angle, which will be referred to as the PC "off-resonance". When the PC is on-resonance, both enhanced excitation and enhanced extraction can impact the fluorescence intensity, while enhanced extraction acts alone when the PC is off-resonance. The impact of enhanced extraction in particular is dependent on the detection instrumentation since the effect relies on radiation of emitted light in specific directions (toward the detector). The microarray scanner used in this study has a large acceptance angle for emitted light, so the effects of enhanced extraction are measurable.

The background intensity of the PC off-resonance is 5.95× higher than the glass slide, and the off-resonance PC noise intensity is 2.92× higher than the glass slide, with a less than 4% coefficient of variation for both measurements over all spots on the devices. This increased background in the PC is due primarily to autofluorescence from the UV-cured polymer structure and PET substrate. The on-resonance PC background intensity is 1.57× the off-resonance PC background, and the average ratio of on-resonance to off-resonance noise intensity is 1.30×. These numbers suggest that only small increases in background fluorescence occur due to high electric fields within the PC. When the PC is on-resonance, its average background intensity is 9.34× the glass background and its average noise intensity is 3.79× the glass noise.

The enhancements observed in the signal intensities are in fact higher than the increased background and noise intensities, which lead to increased SNR. The SNR is the net spot intensity divided by the noise intensity and represents how easily a spot can be differentiated from noise. For the assessment of the SNR enhancement, the data is analyzed in two groups: the three highest concentrations of analyte (40, 200, and 1000 pg/mL) and the two lowest concentrations (8 and 1.6 pg/mL) plus the negative control. The rationale for this division is the fact that the SNR observed on the glass slide is less than 3 for the lower concentrations and control, which indicates the signals cannot be distinguished from noise. At the higher concentrations, the signal intensity is primarily determined by the number of fluorophores on the device surface.

Table 1. Average Signal-to-Noise Ratios of the Immunoassay On All Devices

concentration (pg/mL)	glass slide	PC off resonance	PC on resonance
1000	174 (±66.4)	293 (±58.1)	1060 (±181)
200	37.2 (±17.9)	38.5 (±6.01)	138 (±26.4)
40	5.31 (±2.78)	7.72 (±1.42)	29.9 (±4.96)
8	1.30 (±0.90)	2.39 (±0.53)	8.91 (±1.84)
1.6	0.686 (±0.32)	1.53 (±0.45)	5.75 (±1.41)
negative control	0.338 (±0.20)	1.06 (±0.35)	4.27 (±1.32)

A comparison of the SNR enhancement factors at these concentrations shows the SNR is enhanced by an average factor of 1.40 times on the off-resonance PC relative to the glass slide. The PC SNR is enhanced another 3.69 times on-resonance, which makes the total SNR enhancement of the resonant PC relative to the glass slide a value of 5.14. For the lower concentrations and negative control, the glass slide intensities and off-resonance PC SNRs are lower than 3, but the on-resonance PC has SNRs all greater than 3 (Table 1). In other words, unlike the glass and off-resonance PC, the on-resonance PC performance is not noise-limited at low concentrations, thus making it possible to detect lower concentrations of analyte on the PC. Figure 4 illustrates the enhanced SNR for spots incubated with the lowest concentration of TNF-α (1.6 pg/mL), with an estimated SNR enhancement of over 8 times. This SNR enhancement is one component in lowering the detection limit of the immunoassay, which can be addressed in more detail by an analysis of the complete concentration series.

Concentration Series Analysis. The net signal intensities for each concentration series were fitted to four-parameter logistic curves using ProMAT software and plotted with their fitted curves in Figure 5a. First, the sensitivity, or change in signal per change in concentration, is evaluated for identical scan conditions. By determining the slopes on the fitted curve at each concentration assayed and calculating the ratio of PC to glass slopes, the off-resonance PC sensitivity enhancement was calculated to be 3.86 ± 1.14 and the on-resonance PC sensitivity enhancement was calculated to be 22.6 ± 7.11. While the variation in the sensitivity enhancement is considerable due to the complexity of the curves, these figures clearly illustrate the sensitivity of the assay is increased by the PC. However, the utility of an increased sensitivity is compromised if the assay resolution is negatively affected. For example, the laser intensity can be increased to excite fluorophores more brightly but the observed noise will also increase, altering the sensitivity but having no effect on resolution, where the resolution is defined as three times the noise divided by the sensitivity. The resolution represents the smallest change in concentrations that can be distinguished from noise. In the case of the PC, when the sensitivity of the assay is enhanced, the noise-limited resolution is actually augmented as well. At an assay concentration of 200 pg/mL, within the linear dynamic range of the assay, the resolution of the glass substrate immunoassay is 17.0 pg/mL, while the resolution of the on-resonance PC substrate immunoassay is 2.69 pg/mL. Throughout all concentrations the impact of the off-resonance PC on the resolution is modest, with the PC resolution being 74.1 ± 20.1% of the glass resolution. The on-resonance PC has a much more dramatic effect on the
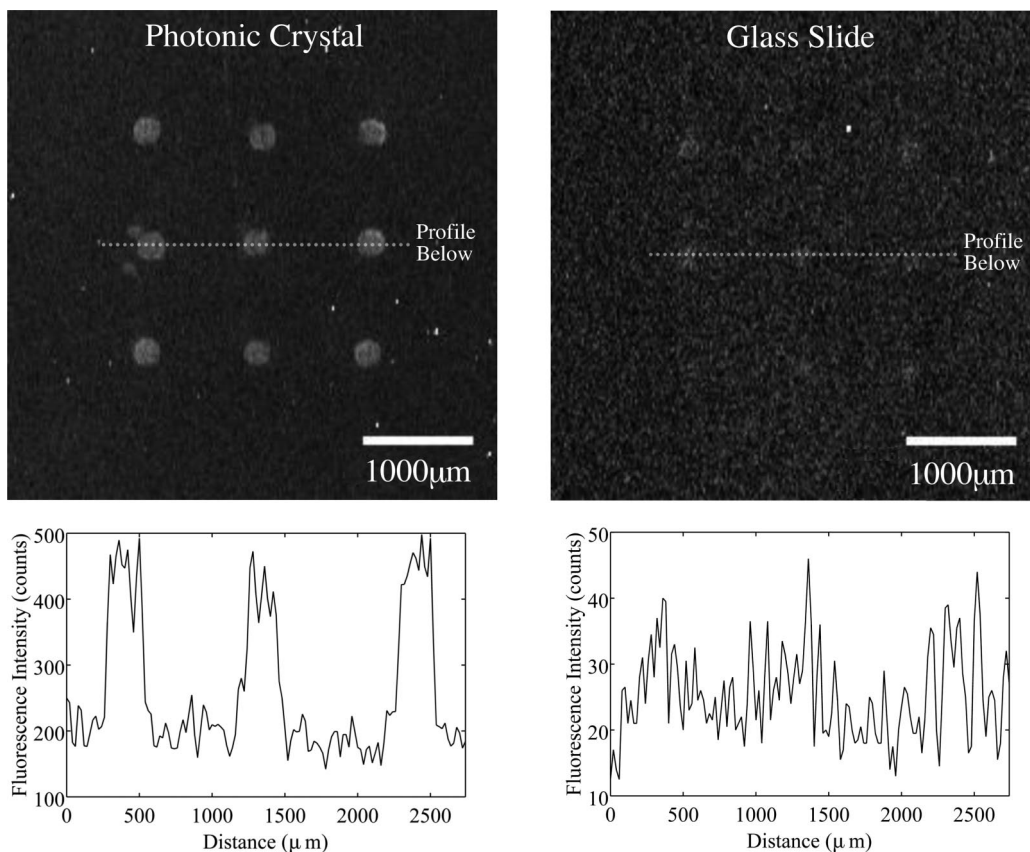
Figure 4. Fluorescence images and associated line profiles from the PC and glass immunoassays at a concentration of 1.6 pg/mL. The fluorescence images are contrast-adjusted for better visualization of the spots. The PC signal-to-noise ratio is ~8 times higher than the ratio for the glass slide immunoassay spots.

resolution—the on-resonance PC resolution through all concentrations is 16.8 ± 6.2% of the glass resolution.

One possible benefit of enhanced resolution with the PC is enhanced limits of detection, which was evaluated by extrapolation during the curve-fitting process with ProMAT. Observation of the lower concentrations of the assay in Figure 5b shows the spot intensities on both the on-resonance and off-resonance PCs are considerably higher than for the glass slide, which reflects the enhanced SNR shown in Figure 4. With a higher sensitivity and enhanced resolution, the PC is expected to show a lower limit of detection. By evaluating the intensity of the negative control plus three times its standard deviation in relation to the fitted curve, ProMAT calculated the lower limit of detection for the glass slide assay was 17.64 pg/mL. The off-resonance PC assay demonstrated a limit of 8.85 pg/mL and the on-resonance PC assay demonstrated a limit of 5.90 pg/mL, representing limits of detection of 50 and 33% of the glass slide limits, respectively. These calculated detection limits represent quantitative limits of detection, or the minimum concentrations that can be accurately quantified by the assay. Concentrations lower than this limit can be differentiated from noise but cannot be accurately quantified.

DISCUSSION

Enhancing the signal from fluorescent molecules is a promising methodology for improving fluorescence-based assays such as the immunoassay demonstrated in this work. Fluorescence of Cy-5 from immunoassay spots on the PC was enhanced by more than 20× relative to a control glass slide. A popular analog to the PC-

enhanced fluorescence approach is metal-enhanced fluorescence, which uses metal structures to enhance fluorescence through enhanced electrical fields or radiative lifetime modification. Metal-enhanced fluorescence has demonstrated a range of enhancement factors in the context of immunoassay experiments, with enhancements as high as 100-fold for rhodamine on silver fractal-like structures[17] and of ~8× for Alexa Fluor-555-labeled IgG's on silver island films.[18] However, the disadvantage of these formats is a lack of uniformity over large areas needed to assay a concentration series; fractal-like structures demonstrate hot spots and silver island films are randomly oriented. The enhanced electric field distribution of the PC in this work has a period on the order of ~500 nm and this periodic pattern covers an entire microscope slide. Thus, the PC is capable of enhancing the fluorescent signal in a reproducible fashion over the entire slide. This distance is more than 1 order of magnitude smaller than the highest resolution for fluorescent microarray scanners as well as the smallest microarray spots, ensuring that a uniform enhancement is achieved for all microspots without any alignment of spots to the substrate. The ability to enhance fluorescence reproducibly over large areas is particularly important for immunoassays since a concentration curve is generated using multiple standard concentrations, which requires multiple sample wells. Furthermore, PCs can be generated inexpensively over microscope slides

(17) Shtoyko, T.; Matveeva, E. G.; Chang, I.-F.; Gryczynski, Z.; Goldys, E.; Gryczynski, I. *Anal. Chem.* **2008**, *80*, 1962–1966.
(18) Zhang, J.; Matveeva, E.; Gryczynski, I.; Leonenko, Z.; Lakowicz, J. R. *J. Phys. Chem. B* **2005**, *109*, 7969–7975.

by nanoreplica molding, so the advantages of enhanced fluorescence can be realized without exorbitant fabrication costs.

This work demonstrates for the first time the application of enhanced fluorescence to a microspot immunoassay, and in examining this application, the practical benefits of enhancing fluorescence at low analyte concentrations can be assessed. In particular, the microarray allows a simple observation of the SNR ratio since large areas of the device do not contain fluorescent signal from the antibody sandwich complex. The assay noise is composed of signal from nonspecific binding onto the substrate, but it also contains signal from the substrate itself since the confocal scanner measures fluorescence 35 μm below the substrate surface. PC-enhanced fluorescence increases the SNR in three ways. First, the electric field from the laser light is enhanced selectively throughout the substrate, including where fluorophores are concentrated. Second, some proportion of light emitted from fluorophores will couple to the structure and be redirected toward the detector, capturing light that would be lost if the assay were performed on glass. Third, a large proportion of the laser light is reflected due to the resonant behavior of the PC, which ensures that the PC substrate fluorescence is excited less than an optically passive substrate such as glass. While these mechanisms of SNR enhancement do not address noise from nonspecific binding, they can decrease the contribution of substrate fluorescence to the SNR. The importance of substrate fluorescence may vary depending on the type of assay performed, but this work demonstrates that increasing SNR does yield performance benefits for the TNF-α microspot immunoassay. In this work, an identical protocol for the immunoassay was performed on glass slides and PCs, but it is also important to recognize that the SNR enhancement may allow for modification of the protocol for more stringent assay conditions. Such conditions could decrease the influence of nonspecific binding while fluorescence enhancement maintains an adequate signal for quantification of very low concentrations of protein.

PC-enhanced fluorescence of Cy-5 yielded a signal from immunoassay spots that was enhanced by more than 20× relative to a control glass slide, with ~4× enhancement from enhanced extraction and 6× enhancement from enhanced excitation. The excitation enhancement of 6× compares favorably with predicted values of 4−7× from RCWA simulation, demonstrating that enhanced excitation can indeed be modeled. Work is currently underway to accurately model enhanced extraction as well in order to precisely predict the impact of modifications to PC designs on the expected enhancement for a given fluorophore. Even without an accurate enhanced extraction model, the ability to simulate the electromagnetic field profile of the PC is extremely valuable in guiding rational design of enhanced excitation, particularly since the spatial field distribution may be engineered for increased performance.

Despite achieving a more than 20× enhancement of the fluorescence intensity from Cy-5 and a SNR enhancement of more than 5×, the PC design used in this work can be further optimized. The fact that the SNR enhancement does not equal the signal enhancement illustrates that noise is enhanced as well as signal, but the PC improves assay performance because the signal is enhanced to a greater degree than the noise (likely a result of enhancing fields selectively in the fluorophore region as well as
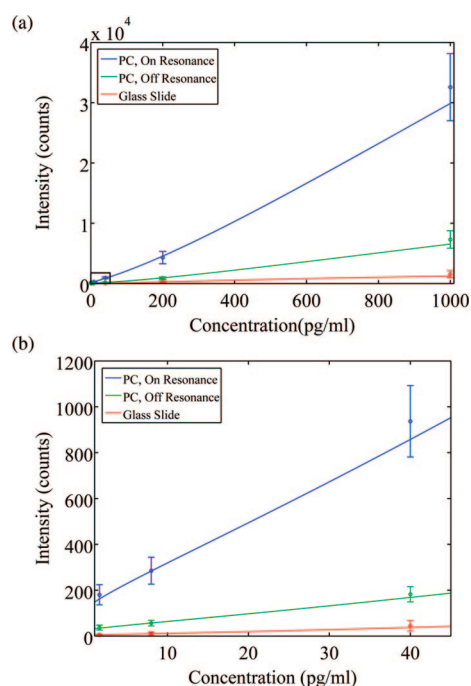

Figure 5. (a) Net signal intensity as a function of TNF-α concentration for the immunoassay performed on the PC on-resonance, the PC off-resonance, and the glass slide. The data points and error bars are included with their fitted logistic curves. (b) The data from (a) of the three lowest assay concentrations.

the reflection of the incident light). However, the SNR enhancement may be improved by either reducing the noise from the substrate or selectively increasing the signal enhancement. One method of reducing substrate noise is by utilizing substrate materials that exhibit less fluorescence at the wavelengths of interest. UV-cured polymer demonstrates higher levels of fluorescence than glass, but it is necessary for the nanoreplica molding process that provides inexpensive fabrication. Alternative materials may be pursued, but materials that cannot be replica molded would require lithography to be performed on every substrate, which adds considerably to the cost per substrate. An additional approach to improved performance is to pursue higher signal enhancements and engineer the high electric field regions to overlap the fluorophores rather than the substrate. This can be achieved by altering the PC dimensions in an effort to reduce the resonance line widths, which are inversely proportional to electric field intensity enhancement and fluorescence of molecules on the PC surface.[9] Alternatively, modeling of label-free PC biosensors shows that regions of high electric field intensity could be biased toward the surface of the device (the fluorophore region) by using a substrate material with a lower refractive index.[19] Thus, the device presented in this work is not an optimized PC; alterations to PC materials can lead to increased signal enhancement and decreased noise enhancement and resonant line width engineering can yield larger signal enhancement factors.

The SNR enhancement of the PC was substantial enough to simultaneously increase the sensitivity, enhance the resolution, and lower the detection limit of the TNF-α immunoassay. The on-resonance PC demonstrated a sensitivity enhancement of more

(19) Block, I. D.; Ganesh, N.; Lu, M.; Cunningham, B. T. *IEEE Sens. J.* **2008**, *8*, 274−280.

than 20× relative to a glass slide, while decreasing the minimum resolvable difference in concentrations by ~85%. This is significant because the sensitivity of the assay (defined as the slope of the concentration curve) can be manipulated by a simple instrumentation change such as altering the PMT gain. However, the noise will increase concordantly in such a case, yielding no gain in resolution. The SNR enhancement allows for an increased fluorescence signal that is higher than a concurrent increase in noise—improving the resolution and detection limit. The quantitative lower limit of detection for the resonant PC was 1/3 the limit of the glass slide. Furthermore, the lowest concentration assayed, 1.6 pg/mL, could be detected (but not quantified) above noise on the PC and not on the glass slide. The improvement of these metrics can be attained without an alteration of the basic instrumentation used for a protein microarray experiment, so this technology should be straightforward to implement by laboratories currently pursuing microarray research. In addition, the PCs are manufactured inexpensively over large areas, so improvements can be attained without significant expense for instrumentation or for the PC substrate.

The cytokine TNF-α plays an integral role in the immune response during infection and has been studied as a biomarker for sepsis, a state of acute inflammation throughout the body that is responsible for more than 100 000 deaths a year in the United States.[20] An evaluation of cytokine concentrations in sepsis diagnosis determined that TNF-α could be a useful biomarker with a cutoff value of 11.5 pg/mL,[21] which is below the limit of detection for the glass slide but not the PC in this study. This cutoff is not much higher than normal physiological TNF-α serum concentrations of 5−10 pg/mL,[22,23] which underscores the importance of resolution—a metric that was significantly improved in the PC relative to the glass slide. While the sensitivity and specificity of TNF-α in sepsis diagnosis is not high enough to warrant its use as a lone biomarker, the addition of other cytokines in the immunoassay may be powerful and is a subject of future study. The protein microarray format lends itself to quantitation of multiple serum proteins at once by spotting capture antibodies to multiple analytes, and accurate, multiplexed cytokine measurement would be a valuable tool in understanding the modulation of the immune system during sepsis.

As the biological role of networks of serum proteins in disease is further studied, protein microarrays can serve as an important tool for researchers who need to assay many quantities simultaneously. PC-enhanced fluorescence is a valuable tool to inexpensively augment the performance of these microarrays. With further improvements in PC performance, the detection limits of these assays can be decreased even further, which may be useful in detecting new biomarkers associated with disease. Decreased detection limits can also enable researchers to monitor not only significant increases in serum proteins such as cytokines but also decreases in their levels as well, which may provide additional, previously unattainable information about sepsis and other complex diseases.

CONCLUSION

A PC resonant at the excitation wavelength for Cyanine-5 was modeled using RCWA and demonstrated enhanced fields upon illumination at the resonant angle. The spatial field profiles suggested at least a 4× enhancement of fluorescence from molecules on the PC surface due to enhanced excitation alone, with the mechanism of enhanced emission likely providing additional fluorescence enhancement. The PC was fabricated using a nanoreplica molding process with UV-curable polymer followed by a deposition of high refractive index dielectric. A fluorescence microarray format immunoassay was performed on the PC and compared with a glass slide with an identical surface chemistry. The resonant PC demonstrated a 5× enhancement of SNR relative to the glass slide, translating to increased resolution for the PC immunoassay and the ability to detect an analyte concentration of 1.6 pg/mL on the PC. In addition, the quantitative limit of detection achieved on the PC was one-third the limit observed on the glass slide. These results demonstrate that a PC-enhanced fluorescence immunoassay can provide better resolution and lower detection limits than an assay on an optically passive substrate.

(20) Carrigan, S. D.; Scott, G.; Tabrizian, M. Clin. Chem. 2004, 50, 1301–1314.
(21) Balc, C.; Sungurtekin, H.; Gurses, E.; Sungurtekin, U.; Kaptanoglu, B. Crit. Care 2002, 7, 85–90.
(22) Aziz, N.; Nishanian, P.; Fahey, J. L. Clin. Diagn. Lab. Immunol. 1998, 5, 755–761.
(23) Scala, E.; Pallotta, S.; Frezzolini, A.; Abeni, D.; Barbieri, C.; Sampogna, F.; Pita, O. D.; Puddu, P.; Paganelli, R.; Russo, G. Clin. Exp. Immunol. 2004, 138, 540–546.